Steady-state level-anticrossing spectra for bound-exciton triplets associated with complex defects in semiconductors

W. M. Chen, M. Godlewski,* B. Monemar, and J. P. Bergman
Department of Physics and Measurement Technology, Linköping University, S-581 83 Linköping, Sweden
(Received 21 March 1989; revised manuscript received 31 October 1989)

A detailed analysis of magnetically induced level-anticrossing (LAC) effects for bound-exciton (BE) triplets associated with isoelectronic complex defects in semiconductors is presented, using rate equations and a spin Hamiltonian approach. It is shown that the observation of the LAC effects is due to nonvanishing microscopic interactions coupling the approaching states. In addition there exists an inequivalency between these states, due to a steady-state excitation mechanism. The hyperfine interactions are proved to be the main static interaction responsible for the LAC effects. Characteristic distinctions between different BE systems (from thermalized to unthermalized) are shown to exist in the vicinity of the LAC field region as well as for high magnetic fields. A good agreement between the treatment developed in the present work and experimental LAC spectra for several complex defects in GaP has been obtained. Useful information about the bound excitons and their associated defects can be extracted by simple steady-state level-anticrossing spectroscopy, i.e., in complete absence of external perturbing radiofrequency or microwave fields.

I. INTRODUCTION

The observations of resonantlike changes in phosphorescence intensity in materials by applying a magnetic field have been mostly attributed to cross-relaxation (CR) effects and level anticrossing (LAC).[1,2] Magnetic cross-relaxation is an irreversible process that provides an important mechanism for energy transfer in the solid state,[1] involving the spin systems of both the guest (impurity) and the "host" (e.g., host material, defect, or another impurity). Magnetically induced LAC, in contrast, does not require the participation of a second spin reservoir, and is observed whenever two coupled levels are brought into coincidence by an external magnetic field.[2] Extensive LAC experiments have been carried out for atoms and molecules[3-8] and for phosphorescent organic crystals,[9-12] ever since the first observation of LAC on the sublevels of the $2\,^2P$ manifold of the Li atom.[13] Similar detailed investigations of LAC phenomena for bound excitons (BE's) in semiconductors are still virtually missing, however, although a few LAC observations have been reported as a complement to studies of optically detected magnetic resonance (ODMR).[14-17]

LAC effects in semiconductors play an important role in, e.g., annihilation and quenching of BE's and other related phenomena. They may also provide valuable structural information about BE's and their associated defects. Recently, the strong influence of LAC effects on ODMR spectra for complex defects in semiconductors has been shown to occur.[18] In this paper, we present a detailed steady-state analysis of LAC effects [in the complete absence of perturbing radiofrequency (rf) or microwave (MW) fields] on BE triplet states associated with neutral complex defects in semiconductors. The formal treatment is developed with the aid of rate equations and a spin-Hamiltonian approach.

The paper is organized in the following way. In Sec. II we exploit the rate equations and the spin Hamiltonian for a BE triplet. Section III contains a detailed discussion and analysis of the LAC effects, in connection with some recently observed experimental results from several isoelectronic complex defects in GaP. The most important conclusions are collected in Sec. IV.

II. RATE EQUATIONS AND SPIN HAMILTONIAN TREATMENT OF LEVEL ANTICROSSINGS FOR SPIN-TRIPLET BOUND EXCITONS

A bound exciton, associated with a neutral complex defect[19] with a strong hole-attractive local potential in a semiconductor, typically has a singlet-triplet (S-T) configuration[20] as the lowest electronic states. The electron-hole (e-h) exchange interaction tends to leave the triplet lowest in energy, with an S-T separation typically much larger than the level splittings induced by other small perturbations, such as Zeeman, fine-structure, and hyperfine-structure interactions.[21] A treatment limited only to the BE triplet consequently seems to be appropriate to explain experimental data, considering the coupling between the singlet and triplet as a perturbation.

The LAC phenomenon for a BE triplet is detected (1) via the changes in intensity or polarization of the photoluminescence (PL) signal (due to the BE annihilation); (2) via the splittings of the BE electronic levels in the vicinity of such avoided crossings. The second case is essentially limited only to these BE's which give rise to well-resolved electronic-transition lines, and the analysis of such LAC spectra is rather straightforward. In this paper we shall concentrate our discussion only on the first case, which is not at all limited as is the second case. However, the analysis of such LAC spectra is not straightforward, and

is still absent in literature for BE's in semiconductors. In order to investigate the changes in intensity or polarization of the PL signal due to the LAC effect, the understanding of the variations in the populations and radiative decay rates for the relevant energy levels is of key importance. The access to this understanding can most conveniently be made by means of a rate-equation treatment and a spin-Hamiltonian formalism.

A. Rate equation for bound-exciton-triplet recombination

The Zeeman-split levels of the BE triplet are shown in Fig. 1 in the presence of a built-in local crystal field (here taken as being of C_{3v} point-group symmetry, for illustration) and an external magnetic field. The rate equations for the population of each sublevel, n_1, n_2, and n_3, respectively, are given by[22,23]

$$\begin{aligned}
\frac{dn_1}{dt} &= G_1 - R_1 n_1 - \frac{n_1}{T_1} \\
&\quad + \frac{(n_1+n_2+n_3)e^{-(E_1-E_2)/kT}}{T_1(1+e^{-(E_1-E_2)/kT}+e^{(E_2-E_3)/kT})} , \\
\frac{dn_2}{dt} &= G_2 - R_2 n_2 - \frac{n_2}{T_1} \\
&\quad + \frac{(n_1+n_2+n_3)}{T_1(1+e^{-(E_1-E_2)/kT}+e^{(E_2-E_3)/kT})} , \qquad (1) \\
\frac{dn_3}{dt} &= G_3 - R_3 n_3 - \frac{n_3}{T_1} \\
&\quad + \frac{(n_1+n_2+n_3)e^{(E_2-E_3)/kT}}{T_1(1+e^{-(E_1-E_2)/kT}+e^{(E_2-E_3)/kT})} .
\end{aligned}$$

Here the generation rates and energies for the sublevels are denoted as G_1, G_2, and G_3, and E_1, E_2, and E_3, respectively. R_1, R_2, and R_3 are the recombination rates for the respective states, including radiative (R_i^r), nonradiative (R_i^{nr}), and transfer rates (R_i^t), etc., where $i=1$, 2, and 3. T_1 is a time constant related to the spin-lattice relaxation for the Zeeman sublevels of the BE triplet; T_1 is here assumed to be the same for the three sublevels.[23] The various terms included in each equation in Eq. (1) are the generation term, the recombination term, the relaxation term, and the thermalization term, respectively.

For steady-state conditions, i.e., $dn_i/dt=0$ with $i=1,2,3$, these equations can be written in a matrix representation as

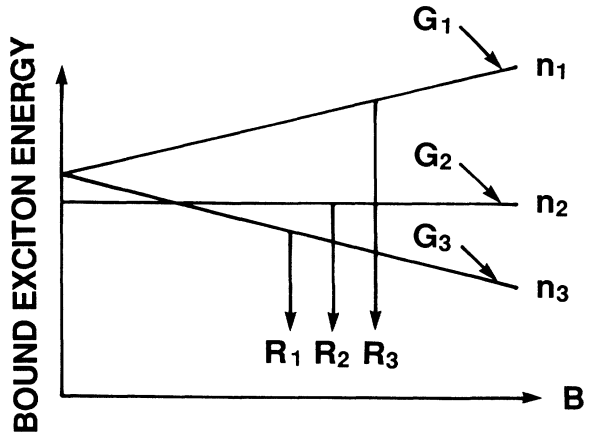

FIG. 1. Schematic picture of Zeeman-split sublevels for a BE triplet in the presence of a local crystal field (here taken as having C_{3v} symmetry with the trigonal axis **z**) and an external magnetic field ($\mathbf{B}\|\mathbf{z}$). The generation rates G_i, recombination rates R_i, and populations n_i for each sublevel are shown; these are in general magnetic field dependent (i.e., dependent on the mixing of the substates, and in addition, in the case of n_i, dependent on the thermal contact between the Zeeman-split sublevels), as defined in the text.

$$\underline{A}\,\underline{N}=\underline{B} , \qquad (2)$$

where

$$\underline{N}=\begin{bmatrix} n_1 \\ n_2 \\ n_3 \end{bmatrix}, \quad \underline{B}=\begin{bmatrix} -G_1 \\ -G_2 \\ -G_3 \end{bmatrix}$$

and

$$\underline{A}=\begin{bmatrix} WA_{12}-X_1 & WA_{12} & WA_{12} \\ W & W-X_2 & W \\ WA_{23} & WA_{23} & WA_{23}-X_3 \end{bmatrix} ,$$

with $A_{12}=e^{-(E_1-E_2)/kT}$, $A_{23}=e^{(E_2-E_3)/kT}$, $1/W=T_1(1+A_{12}+A_{23})$, $X_i=R_i+1/T_1$, where $i=1,2,3$. Exact solutions can be obtained by performing transformations of the form

$$\underline{N}=\underline{A}^{-1}\underline{B} , \qquad (3)$$

or explicitly,

$$\begin{aligned}
n_1 &= \frac{1}{\Delta}\{G_1R_2X_3 + A_{12}[G_1R_2X_3+(1/T_1)(G_2X_3+X_2G_3)] + A_{23}G_1X_2R_3\} , \\
n_2 &= \frac{1}{\Delta}\{[X_1G_2X_3+(1/T_1)(G_1X_3+X_1G_3)] + A_{12}R_1G_2X_3 + A_{23}X_1G_2R_3\} , \qquad (4) \\
n_3 &= \frac{1}{\Delta}\{X_1R_2G_3 + A_{12}R_1X_2G_3 + A_{23}[X_1X_2G_3+(1/T_1)(G_2X_1+X_2G_1)]\} ,
\end{aligned}$$

where $\Delta = X_1R_2X_3 + A_{12}R_1X_2X_3 + A_{23}X_1X_2R_3$.

In order to illustrate the population distributions among the BE-triplet sublevels, we take the examples of a completely thermalized and an unthermalized case, respectively.

(i) In the thermalized case, i.e., $1/T_1 \gg R_{1,2,3}$, we obtain from Eq. (4) the population for each sublevel as

$$n_1 = \frac{A_{12}(G_1+G_2+G_3)}{R_2+A_{12}R_1+A_{23}R_3} ,$$
$$n_2 = \frac{(G_1+G_2+G_3)}{R_2+A_{12}R_1+A_{23}R_3} , \quad (5)$$
$$n_3 = \frac{A_{23}(G_1+G_2+G_3)}{R_2+A_{12}R_1+A_{23}R_3} ,$$

i.e.,

$$n_1 = n_2 e^{-(E_1-E_2)/kT} ,$$
$$n_3 = n_2 e^{(E_2-E_3)/kT} . \quad (6)$$

The triplet is thermalized, as is obvious from the fact that the BE population distribution within the triplet follows the Boltzmann statistics.

(ii) In the unthermalized case, i.e., $R_{1,2,3} \gg 1/T_1$, we obtain from Eq. (4) the populations for each sublevel as

$$n_1 = G_1/R_1 ,$$
$$n_2 = G_2/R_2 , \quad (7)$$
$$n_3 = G_3/R_3 .$$

If $R_1, R_3 \gg R_2$ (i.e., in the case of a slower emitting sublevel 2), $n_2 \gg n_1, n_3$. The population distribution does not follow the Boltzmann statistics, as expected for an unthermalized BE triplet.

B. Spin-Hamiltonian formalism

As is evident from a number of ODMR studies (see Ref. 21 and references therein), the properties of the BE triplet have, in many cases, been quite successfully described by a spin Hamiltonian of the form[24]

$$H_S^{BE} = \mathbf{S}\cdot\underline{D}\cdot\mathbf{S} + \mu_B\mathbf{S}\cdot\underline{\mathbf{g}}\cdot\mathbf{B} + \mathbf{S}\cdot\underline{\mathbf{A}}\cdot\mathbf{I} + \sum_i \mathbf{S}\cdot\underline{\mathbf{A}}_i\mathbf{J}_i , \quad (8)$$

where $\mathbf{S}$ denotes the electronic spin of the BE ($S=1$ for a BE triplet), $\mathbf{I}$ and $\mathbf{I}_i$ are the nuclear spins of the defect and its ligand atom(s), respectively. μ_B is the Bohr magneton, and $\mathbf{B}$ the external magnetic field. $\underline{\mathbf{g}}$, $\underline{D}$, and $\underline{\mathbf{A}}$ are the g tensor, the fine-structure tensor, and the hyperfine-structure tensor, respectively. The basis set of the electronic spin wave functions may be naturally chosen as the spin $S=1$ basis $|S,M\rangle$ (where $S=1$ and $M=+1,0,-1$), a subbasis derived from the basis set of the lowest BE singlet-triplet states, e.g., direct products of the spinors for the bound electron and the bound hole.

Knowing the proper basis spin wave functions (including the electron and nuclear part) and the relevant spin Hamiltonian, the eigenenergies and the eigenstates can easily be obtained by a complete diagonalization of the spin-Hamiltonian matrix. The effects of mixing of the wave functions by the various perturbations given in the spin Hamiltonian are reflected directly from the form of the eigenfunctions, which are in principle linear combinations of the unperturbed basis wave functions, i.e.,

$$\psi_i = \sum_{M=-1}^{+1} a_{iM}|1,M\rangle , \quad (9)$$

where $i=1,2,3$.

C. Level-anticrossing effects

The photoluminescence intensity of each sublevel is proportional to the population and the radiative recombination rate for the level,

$$L_i = \alpha R_i^r n_i , \quad (10)$$

where α is a proportionality constant, and $i=1,2,3$. The LAC effects are monitored, in its steady-state behavior, by the changes of the PL intensity (either the total intensity or for differentially polarized light) versus the external static magnetic field, i.e., L_i-$\mathbf{B}$ relations. Therefore, variations of the radiative recombination rates and populations for the different sublevels in the magnetic field play key roles in determining the strengths of the LAC signals.

The detection of differently polarized light, which is often a much more sensitive technique, requires the knowledge of the polarization for each level. This may in principle be obtained by inspection of the wave function for each level, since the absolute square of the coefficient a_{iM} from Eq. (9) is proportional to the probability for the BE to be found in the state $|1,M\rangle$, provided that the polarization of this state is known.[25] More explicitly,

$$n_i = \sum_{M=-1}^{+1} n_{iM} \quad (11)$$

for the sublevel i, and

$$n_{iM} = |a_{iM}|^2 n_i . \quad (12)$$

The PL intensity of level i can be written in the form

$$L_i = \sum_{M=-1}^{+1} L_{iM} = \alpha \sum_{M=-1}^{+1} R_M n_{iM} , \quad (13)$$

where R_M refers to the radiative fraction of the recombination rate, responsible for the BE transition from $|1,M\rangle$ to the singlet ground state. The recombination transitions of a BE are in general spin dependent,[25] and the above description in terms of spin polarizations is consequently appropriate. From Eqs. (10)–(13), a reformed expression for the total radiative recombination rate for the level i can be obtained as

$$R_i = \sum_{M=-1}^{+1} R_M |a_{iM}|^2 . \quad (14)$$

Therefore, the radiative recombination rate R_i could be estimated from the knowledge of the mixing of the wave functions among the triplet substates, i.e., the (magnetic)-field-dependent parameters a_{iM}, together with

the field-independent parameters R_M. The latter are uniquely determined by the symmetry of the corresponding BE state in the absence of a magnetic field, if field-dependent coupling of the triplet to its excited states is negligible.[25] These parameters serve as fitting parameters in the analysis of the experimental results.

In practice, when a LAC experiment is done, one works, in most cases, in either the Faraday configuration or in the Voigt configuration. A corresponding analysis should be made, depending on which configuration is used. Often one considers the polarizations with respect to the external magnetic field, so that the quantization axis is naturally chosen along the magnetic field. Therefore, a proper transformation of the coordinates (or basis set of spin wave functions) between the defect-coordinate system and the magnetic-field-coordinate system is usually required. All inequivalent sites of a given defect should also be taken into account in the analysis.

III. DISCUSSION

After the derivation of the relation for the PL intensity (resulting from the BE recombination) as a function of the magnetic field, a detailed discussion as well as a proper analysis of various aspects of the LAC effects will be attempted below.

A. Level crossing (LC) versus level anticrossing (LAC)

An important question is whether the experimentally observed changes in PL intensity or polarization changes in the PL intensity, are due to the level crossing (between noncoupled levels) or level anticrossing (avoided crossing between interacting states). The relevance of this question derives at least partly from the typical absence of resolved hyperfine (HF) structure in ODMR spectra of complex defects in semiconductors. Such HF interaction is expected to cause an avoided crossing due to its function in coupling the states. To identify the nature of the states in the vicinity of the crossing, we assume there exist off-diagonal matrix elements, $V=\langle 1,M|H'|1,K\rangle$, $M\neq K$, induced by some sort of static perturbations H', where the magnitude of V is to be determined. The effect of V on the PL intensity and polarization of the BE recombination is investigated for different cases (varying from a thermalized to an unthermalized system), when the magnetic field is along one of the principal axes of the defect (in this case the effect becomes more significant and therefore this configuration is customarily used in LAC experiments). A plot of the induced signal $L_{\sigma-}$-$L_{\sigma+}$ in such a case is shown in Fig. 2,[26] with the aid of a computer program based on the theoretical background discussed in the previous section. It is clearly shown that a change in the polarization of the PL emission corresponds to a nonvanishing interlevel coupling, so that it is indeed a LAC effect. It is further shown (Fig. 2) that the magnitude of the LAC signals are proportional to the coupling strength V, as long as this perturbation does not dominate over the main interactions for the BE, such as the fine-structure term and the electronic Zeeman interaction. The flattening and further decreasing LAC signal in the region of strong V for the dashed curves and when $|V|\neq 0$ for the solid curves is mainly attributed to a change in the sense of polarizations, since V is no longer a small perturbation in this case, and also due to the broadening of the LAC signal, which transfers some intensity of the signal at the LAC field to its vicinity.

B. Variations of the LAC spectra in relation to the BE properties

The influence of various parameters for the BE (such as R_M, G_M, and T_1) on the appearance of LAC spectra can be investigated in detail with the aid of the methods described in the previous section. As a simple illustration, we discuss below the changes in the difference in intensity of circularly polarized light, i.e., $\Delta(L_{\sigma-}-L_{\sigma+})$, in the vicinity of the LAC region for two different cases: a thermalized and an unthermalized BE-triplet system of

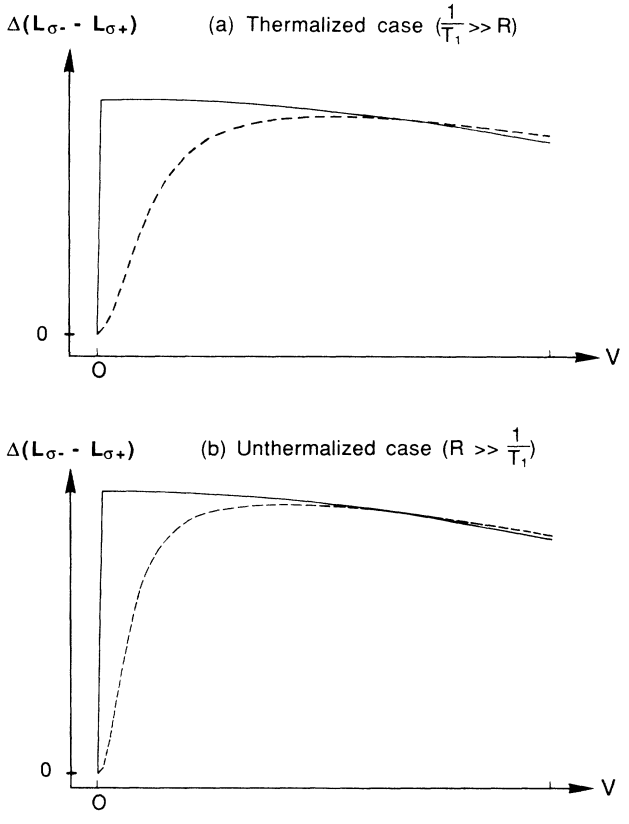

FIG. 2. Effect of the interlevel coupling (V) on the difference of the circular polarizations ($L_{\sigma-}-L_{\sigma+}$) for the PL emission, due to triplet-BE recombination, in (a) a thermalized, and (b) an unthermalized case. The magnetic field is set at the formal level-crossing (LC) field point (solid curve) in the absence of an interlevel coupling (when $V=0$), or in its vicinity (dashed curve), and is along the trigonal axis of the BE system with C_{3v} symmetry ($D>0$, see Fig. 1). It is clearly shown that a change of $L_{\sigma-}-L_{\sigma+}$ is observed only when there exists a nonvanishing interlevel coupling, i.e., it is entirely due to a LAC effect. An ideal level crossing results in no such change.

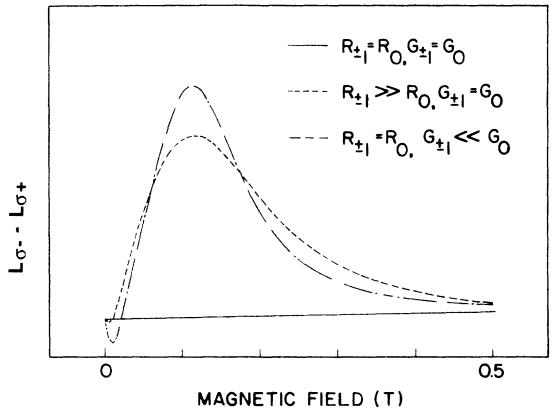

FIG. 3. Effects of generation rates and recombination rates on the LAC spectra, provided that there exists a nonvanishing interlevel coupling between the sublevels of the BE triplet. It is shown that the LAC phenomenon is observed only if there exists some inequivalence between the approaching sublevels, such as different generation rates or different recombination rates. An unthermalized BE triplet of C_{3v} symmetry with $D>0$, when **B** is along the trigonal axis, is chosen as an example in the figure. $G_{\pm1}$, G_0, $R_{\pm1}$, and R_0 are the corresponding quantities for the unperturbed states, with their subscripts ±1 and 0 for $|1,\pm1\rangle$ and $|1,0\rangle$, respectively. In the presence of the interlevel coupling, the relevant quantities for the sublevels (R_i and G_i, $i=1,2,3$) are field dependent, i.e., dependent on the mixing of wave functions.

C_{3v} point-group symmetry, when the magnetic field is along the trigonal axis z. It is assumed in the following discussion that the recombination rate R_i is mainly contributed by its radiative part, i.e., nonradiative contributions are neglected, which is likely to be the case for neutral isoelectronic complexes.

(i) In the thermalized case ($1/T_1 \gg R_{1,2,3}$), one readily obtains from Eq. (4)

$$\Delta(L_{\sigma-}-L_{\sigma+})\approx\frac{\alpha R_3(A_{23}-1)(G_1+G_2+G_3)}{2(R_2+A_{12}R_1+A_{23}R_3)} \quad (15)$$

for a LAC between level 2 and level 3 [E_0 and E_{-1} in the high-(magnetic)-field limit, respectively]. A nonzero signal is expected, since $A_{23}=e^{(E_2-E_3)/kT}$ differs from 1 for an avoided crossing (i.e., $E_2\neq E_3$).

(ii) Similarly, in the unthermalized case ($R_{1,2,3} \gg 1/T_1$) one obtains from Eq. (4)

$$\Delta(L_{\sigma-}-L_{\sigma+})\approx\frac{\alpha(R_3G_2-R_2G_3)}{2R_2} \quad (16)$$

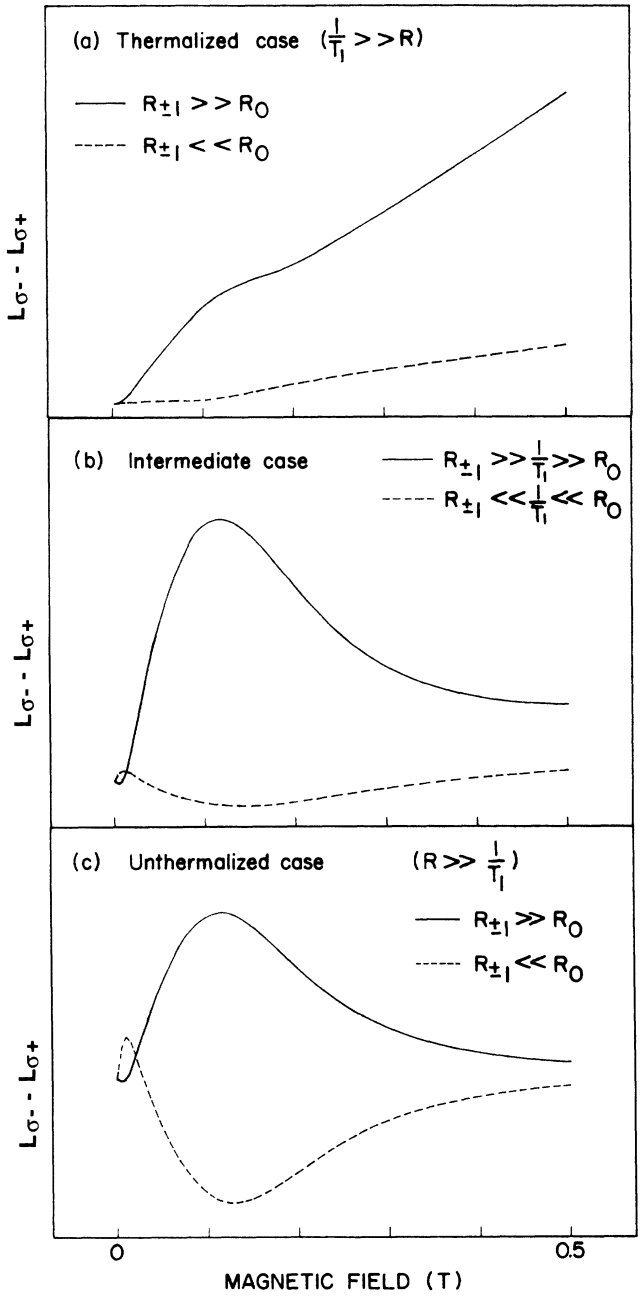

FIG. 4. LAC spectra for (a) thermalized, (b) intermediate, and (c) unthermalized BE triplets, showing clearly characteristic distinctions between these BE triplets in the vicinity of the LAC region as well as at high magnetic fields. The generation rate for each level within the BE triplet is here assumed to be the same, as an example.

TABLE I. A synopsis of LAC effects for different BE triplets, where G is the generation rate, R is the recombination rate, and V is the interlevel coupling term.

BE-triplet properties	Same G and same R for the sublevels or $V=0$	Different G and/or different R for the sublevels, and $V\neq0$	
		weak V	strong V
unthermalized	no	weak	very strong
thermalized	no	very weak	strong

for an LAC between level 2 and level 3. A large variation in $L_{\sigma-}-L_{\sigma+}$ is predicted if $R_3G_2 \neq R_2G_3$.

A synopsis of the LAC effects for different cases of BE systems is given in Table I, and is also schematically demonstrated in Figs. 3 and 4, by numerical computer simulations using the methods described in the previous section. It is shown in Fig. 3 that in order to observe a LAC there must exist some inequivalence between the approaching sublevels, such as different generation rates or different recombination rates, which leads to a difference in their populations. In Fig. 4, quite different LAC spectra are observed for BE systems of different categories, e.g., for a thermalized BE triplet versus an unthermalized BE triplet. Characteristic distinctions are also clearly seen in Fig. 4 between these BE triplets in the high magnetic field region, as will be discussed below in details. The linewidth of the LAC resonantlike peak is shown in scale with the coupling strength V, as can be seen in Fig. 5. It is proved from Fig. 4 that stronger LAC signals are generally expected for the unthermalized BE triplet in comparison to that for the thermalized BE triplet, as can also be found from an inspection of Eqs. (15) and (16).

In Fig. 6, we show magnetic-field-induced changes in the difference of circularly polarized light when the magnetic field is parallel or perpendicular to the defect trigonal axis, respectively. In the former case a LAC is expected, as has been discussed above. In the latter case, no LAC is observed, as can be predicted from the Zeeman-split energy scheme, except a nonresonant overall increase. This commonly observed background signal is induced by the symmetry-breaking effects by the magnetic field (from C_{3v} to C_{1h} in this case), magnetic-field-induced changes in recombination rates for the magnetic sublevels, and also partly by the magnetic-field-induced depopulation of the upper-lying sublevels in the case of a triplet where there exists partial thermalization between the sublevels.

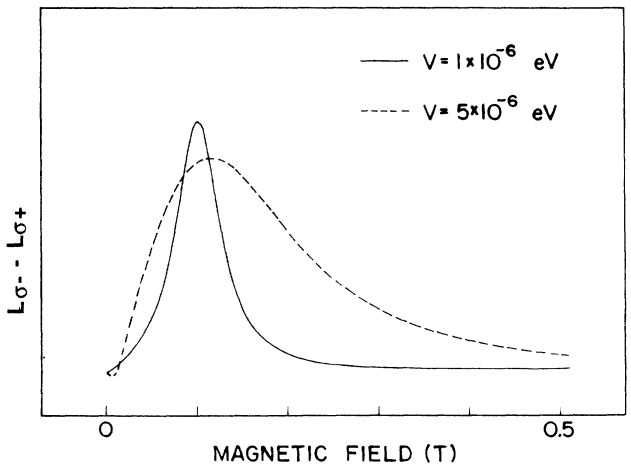

FIG. 5. LAC spectra for different interlevel coupling strengths. The linewidth of the LAC resonancelike peak is shown to be proportional to the interlevel coupling strength. An unthermalized BE triplet is taken as the specific example shown in the figure.

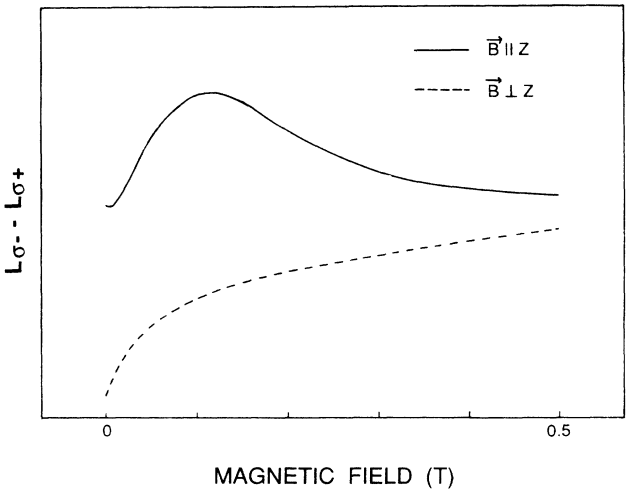

FIG. 6. Magnetic-field-induced changes in $(L_{\sigma-}-L_{\sigma+})$ when **B** is parallel (solid curve) and perpendicular (dashed curve) to the trigonal axis of a BE-triplet system with C_{3v} symmetry (Fig. 1) in the presence of a nonvanishing interlevel coupling. In the first case (solid curve), a strong LAC is expected to occur due to the closely approaching sublevels. In the second case, no such tendency occurs, and no resonancelike LAC is present. Instead, a broad nonresonant background signal is observed, resulting from the symmetry-breaking effects. The BE triplet is here chosen as partly unthermalized.

C. Variations of the total photoluminescence intensity or polarization in the high magnetic field limit in relation to the BE properties

As an example, we discuss the behavior of the difference of the circularly polarized components of the photoluminescence (PL) signal (i.e., $L_{\sigma-}-L_{\sigma+}$) in the high magnetic field limit for a thermalized and an unthermalized BE triplet of C_{3v} symmetry, respectively, when the magnetic field is along the trigonal axis **z**. The same assumption on the recombination rates as that in the previous subsection is used.

(i) In the thermalized case ($1/T_1 \gg R_{1,2,3}$), one obtains from Eq. (4)

$$L_{\sigma-}-L_{\sigma+} \approx \frac{\alpha(A_{23}R_3-A_{12}R_1)(G_1+G_2+G_3)}{R_2+A_{12}R_1+A_{23}R_3} . \quad (17)$$

In the limit $kT \gg \mu_B gB$, which is true in our experiments when $B < 1T$, $L_{\sigma-}-L_{\sigma+}$ scales with the magnitude of the magnetic field. This can easily be visualized, if one considers the increasing difference in populations between the E_{-1} and E_{+1} sublevels with the increase of the magnetic field for a thermalized BE triplet.

(ii) The corresponding result in the unthermalized case ($R_{1,2,3} \gg 1/T_1$), obtained from Eq. (4), is simply

$$L_{\sigma-}-L_{\sigma+} \approx \alpha(G_3-G_1) , \quad (18)$$

which is not strongly magnetic field dependent, at least not explicitly. This is expected, since the increase of sublevel splitting does not cause any severe population

transfer between the sublevels for an unthermalized BE triplet.

There is, therefore, a characteristic distinction between these two BE triplets in their high field behavior. A thermalized BE triplet has a stronger field-dependent character in the polarization properties of the emitted light than in an unthermalized BE triplet, as has been exclusively shown in Fig. 4. This particular behavior, in turn, serves as a useful probe to extract information on the thermalization properties for BE triplets from experimental data.

D. Some experimental LAC results

In Fig. 7 are shown some experimental LAC spectra of the BE triplets associated with the characteristic orange luminescence (COL) in Cu-diffured GaP, (Cu-C), (P_{Ga}-Cu_{Ga}), (P_{Ga}-A), and (P_{Ga}-B) centers in GaP, respectively. The details about sample preparation and optical studies can be found in Refs. 17 and 27–29. The LAC spectra were obtained in the Faraday configuration, employing a magnet attached to a modified Bruker 200D-SRC ESR spectrometer. ($L_{\sigma-} - L_{\sigma+}$) signals were collected by an S-20 photomultiplier or a North Coast EO-817 Ge detector, with the aid of a 50-kHz photoelastic modulator and a Jobin-Yvon 0.25-m grating monochromator. The sample temperature could be varied from room temperature down to 2 K.

As can be seen already by a simple inspection of the figures, good qualitative agreement has been achieved between the experimental results and the theoretical expectations. Numerical simulations have been performed with the aid of the theoretical treatment given in this work by considering all inequivalent sites of a given defect, which provides useful information about the BE and its associated defect center. It is concluded that the BE triplets associated with the (P_{Ga}-A) and (P_{Ga}-B) complexes belong to the class of partially thermalized systems at somewhat elevated temperatures, as can be seen by their characteristic field-dependent LAC spectra [Figs. 7(d) and 7(e)] at high magnetic field. The BE triplets for the (Cu-C) and (P_{Ga}-Cu_{Ga}) complexes, on the other hand, are classified as being unthermalized at low temperature, as can be visualized by nearly field-independent LAC spectra [Figs. 7(b) and 7(c)] at high magnetic field. The absence of any LAC effect on the COL center indicates either that the inequivalence in steady-state excitation process between the BE-triplet sublevels is undetectable, or that the LAC occurs at a higher magnetic field than that reached by the present magnet, meaning that the zero-field splitting is very large, as actually predicted by Zeeman measurements on the same defect.[30] The possibility of a vanishing interlevel interaction can be ruled out, however, since it is believed that the COL BE-triplet wave function is rather localized, supported by its large exchange-interaction-induced singlet-triplet splitting of about 21 meV.

In addition to the thermalization properties, additional valuable information such as the fine-structure interaction, principal axes and consequently the symmetry of the complex defect, microscopic coupling effects (mixing of the wave functions), etc., can also be extracted from the LAC measurements.

To visualize the principle of the method, we resort to a simple quantum-mechanical approach, where the

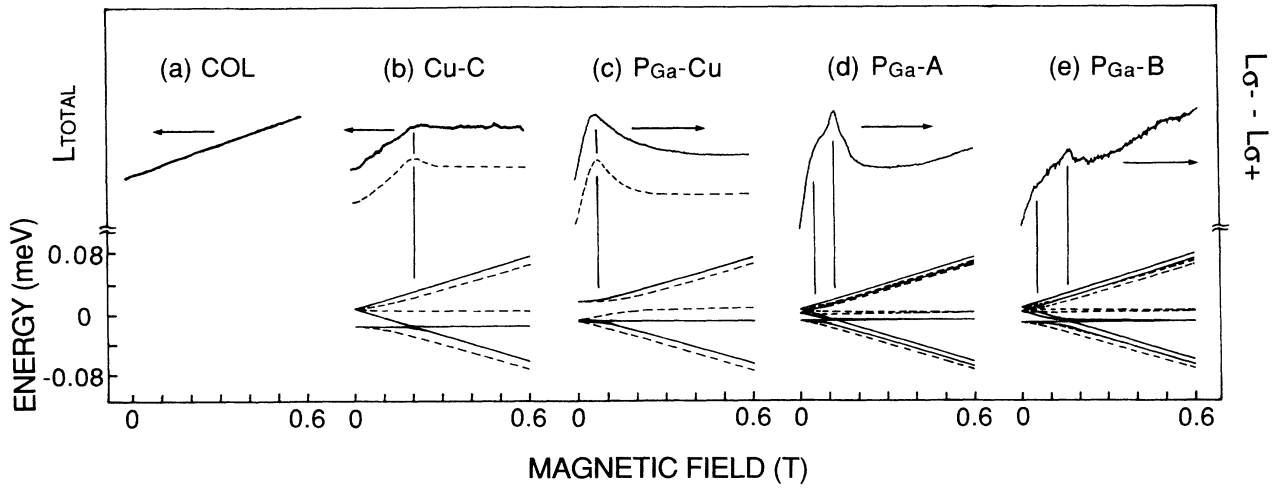

FIG. 7. Experimental LAC spectra (solid curves in the upper part) of the BE triplets associated with (a) COL (at 4 K); (b) (Cu-C) (at 4 K, $\mathbf{B}\|\langle 111\rangle$); (c) ($P_{Ga}$-$Cu_{Ga}$) (at 4 K, $\mathbf{B}\|\langle 001\rangle$); (d) ($P_{Ga}$-$A$) (at 25 K, $\mathbf{B}\|\langle 111\rangle$); and (e) ($P_{Ga}$-$B$) (at 50 K, $\mathbf{B}\|\langle 111\rangle$) centers in GaP. The dashed curves in the upper part of the figure show some of the computer-simulated LAC spectra. The computer-generated Zeeman-split energy diagrams for the corresponding BE triplets are also shown, where the solid and dashed lines represent inequivalent sites of the defect with respect to the magnetic field direction. The vertical lines indicate the field regions where strong LAC occurs. The evaluated parameters are given in Table II.

eigenenergies and eigenstates for two formally degenerated states (e.g., level 1 and 2) can be expressed as

$$E_{1,2}=\tfrac{1}{2}(H_{11}+H_{22}) \pm\tfrac{1}{2}[(H_{11}-H_{22})^2+4|H_{12}|^2]^{1/2} , \quad (19)$$

$$\psi_1=\cos(\beta/2)|\varphi_1\rangle+\sin(\beta/2)|\varphi_2\rangle , \quad (20)$$

$$\psi_2=-\sin(\beta/2)|\varphi_1\rangle+\cos(\beta/2)|\varphi_2\rangle , \quad (21)$$

with $\tan\beta=2H_{12}/(H_{11}-H_{22})$. H_{ij} denotes the matrix elements of the spin Hamiltonian Eq. (8). φ_i is the unperturbed eigenstate for the level i when the off-diagonal coupling H_{ij} $(i\neq j)$ (which corresponds to the notation V used above) vanishes. As can be seen from Eq. (20), the strongest mixing of states and consequently the strongest LAC signal occur when $\beta=\pi/2$, i.e., when $\tan\beta\rightarrow\infty$. This corresponds to an ultimate approach of the two levels ($H_{11}\approx H_{12}$), occurring only when the external magnetic field **B** is along one of the principal axes of a defect. The field position can be determined theoretically by the spin Hamiltonian Eq. (8) to be, e.g.,

$$B=\frac{1}{\mu_B g_z}\left[\left[\frac{3}{2}D_z\right]^2-\left[\frac{D_x-D_y}{2}\right]^2\right]^{1/2} \quad (22)$$

when $\mathbf{B}\|\mathbf{z}$ if the hyperfine interactions can be treated as small perturbations.[18] By performing angular-dependence studies of LAC spectra, therefore, one can obtain the principal axes of the corresponding defect as well as the symmetry. Knowing the LAC fields of such LAC spectra, information about the fine-structure interaction (**D** tensor) and g values of the defect can be extracted, e.g., by Eq. (22) if $\mathbf{B}\|\mathbf{z}$. It should be pointed out that the LAC fields determine only the relation between the components of the D and g tensors in this case. Unique determination of these tensors can be done, however, when a detailed analysis of the angular dependence of the LAC spectra has been carried out. This is due to the fact that the fine structure and the electronic Zeeman terms play quite different roles in the mixing of wave functions, e.g., coupling to different states, and so in the resulting polarization. A computer-aided evaluation is therefore needed in practice, especially when contributions of all inequivalent sites of the defect are taken into account. Such an attempt has been carried out for the BE triplets shown in Fig. 7, and some of the results are shown in Table II. The Zeeman-split energy diagrams for these BE triplets are also shown in Fig. 7, by using the parameters obtained in the analysis of the LAC spectra. Good agreement has been found between these values and that obtained by ODMR studies.[17,28,29] In a case when the LAC effect is absent, such as the COL BE, no corresponding spin-Hamiltonian parameters could be obtained. The accuracy of the spin-Hamiltonian parameters obtained by such a method is limited by the linewidth of the LAC signal, which is proportional to the interlevel coupling V, as seen by Eqs. (20) and (21) and the spin Hamiltonian, i.e.,

$$\frac{\Delta B}{B}\sim\frac{V}{\mu_B g B} . \quad (23)$$

The so-induced error bars for the spin-Hamiltonian parameters are estimated and are given in Table II.

In the last two cases in Fig. 7 for the (P_{Ga}-A) and the (P_{Ga}-B) BE triplets, the central hyperfine (CHF) interactions are so large that they have been readily indicated by the structure appearing in the LAC spectra. From a careful analysis the CHF $\underline{\mathbf{A}}$ tensor can be estimated, as well as the nuclear spin $I=\frac{1}{2}$ of the defect atom which leads directly to the P_{Ga} antisite as part of the defect giving rise to the dominant local potential. In this case, the CHF term is included in the unperturbed spin Hamiltonian. The microscopic interlevel coupling V is then introduced by other smaller perturbations, such as the ligand hf interactions.

There remain some open questions in this analysis, however. The main question is what effects are causing the inequivalence between the sublevels which makes the LAC spectra detectable, i.e., whether it is a difference in

TABLE II. Evaluated parameters for a number of BE triplets in GaP from LAC spectra. The asterisk denotes that the apparent symmetry for the P_{Ga}-Cu_{Ga} defect is C_{2v}, but the true symmetry should be C_{1h} in this case, considering the inequivalence in the substituting atoms.

Parameters		Cu-C	P_{Ga}-Cu_{Ga}	P_{Ga}-A	P_{Ga}-B
Principal axis z		⟨111⟩	⟨001⟩	⟨111⟩	⟨111⟩
Symmetry		C_{3v}	C_{2v}*	C_{3v}	C_{3v}
g tensor	g_z	2.0±0.2	2.0±0.2	2.0±0.1	2.0±0.1
D tensor (10^{-5} eV)	D_z	1.6±0.2	1.0±0.2	0.7±0.1	1.0±0.1
A tensor (10^{-5} eV)	A_z			0.6±0.1	0.6±0.1
V (10^{-5} eV)		~0.13	~0.10	~0.05	~0.05
thermal behavior		unthermalized (at 4 K)		partially thermalized (at 25 K)	(at 50 K)

the generation rates or a difference in the recombination rates that is responsible. A definite identification of the relative importance of these two different contributions requires a detailed future study of the sublevels by time-resolved optical spectroscopy. Such data do not yet exist for triplets in semiconductors. Therefore we shall not attempt to determine quantitatively the dynamical time constants for the BE triplets studied in this work, based solely on steady-state LAC spectroscopy. For the same reason, the computer-simulated LAC spectra shown in Fig. 7 are just for illustration, assuming $G_{\pm 1}=G_0, R_{\pm 1}/R_0>10, R_0/(1/T)_1>10$.

E. Origin of the interactions responsible for the LAC effects

The possible origin of the interactions responsible for the LAC effects is naturally sought mainly among the perturbations given in the spin Hamiltonian Eq. (8), namely Zeeman, fine-structure, and hyperfine interactions. To estimate conveniently the relative importance of the various perturbations, we rewrite the spin Hamiltonian Eq. (8), e.g., for a C_{3v} symmetry, specifically, in a new coordinate system (x',y',z'), defined by $\mathbf{z}'=\mathbf{B}/B$, $y'=\mathbf{z}\times\mathbf{z}'/|\mathbf{z}\times\mathbf{z}'|$, and $\mathbf{x}'=\mathbf{y}'\times\mathbf{z}'$, where $\mathbf{z}$ is the trigonal axis of the defect, into

$$
\begin{aligned}
H_S=&\tfrac{1}{2}\mu_B\cos\theta\sin\theta(g_\perp-g_\parallel)(S'_+ +S'_-)+\mu_B B(g_\perp\sin^2\theta+g_\parallel\cos^2\theta)S'_z\\
&+\tfrac{1}{2}D[S'^2_z-\tfrac{1}{3}S(S+1)](3\cos^2\theta-1)-D(S'_zS'_x+S'_xS'_z)\cos\theta\sin\theta\\
&+\tfrac{1}{4}D(S'^2_+ +S'^2_-)\sin^2\theta+\tfrac{1}{4}[2A_\perp+(A_\parallel-A_\perp)\sin^2\theta](S'_+I'_- +S'_-I'_+)\\
&+\tfrac{1}{4}(A_\parallel-A_\perp)\sin^2\theta(S'_+I'_+ +S'_-I'_-)+(A_\perp\sin^2\theta+A_\parallel\cos^2\theta)S'_zI'_z\\
&-(A_\parallel-A_\perp)\cos\theta\sin\theta(S'_zI'_x+S'_xI'_z)\ ,
\end{aligned}
\tag{24}
$$

where the ligand hyperfine interactions are not included, for brevity.

The possible contributions to the coupling effects (via operators S'_+, S'_- or equivalently S'_x, S'_y) from the Zeeman term and the fine-structure interaction when the magnetic field is along the trigonal axis $\mathbf{z}$, are induced by the misalignment of the crystal off the direction of the magnetic field in the experiment (quite common in practice). This possible misalignment (typically within $\pm 2^0$) leads to a magnitude of the coupling parameter V of the order well below 10^{-7} eV, if originating from the Zeeman and fine-structure interactions for the cases in GaP shown above. This was done by taking into account the relevant off-diagonal terms in the spin Hamiltonian Eq. (24). These values are usually much lower than that estimated from the best fit to the LAC experimental results, however. The main contribution to the LAC effects is, consequently, resulting from the hyperfine interactions. This conclusion is consistent with the ODMR linewidth observed, which is mainly due to unresolved hyperfine and ligand hyperfine interactions. This is in turn evident from the narrower ODMR linewidth observed at zero magnetic field, due to the absence of the first-order hyperfine-induced broadening effect. Other coupling mechanisms, such as phonon-related perturbations, are assumed to be negligible under our experimental conditions.

IV. CONCLUSIONS

In this work, a detailed analysis of the level-anticrossing effects for BE triplets associated with neutral complex defects in semiconductors is presented, with the aid of rate equations and a spin-Hamiltonian approach. It has been explicitly shown that the LAC phenomenon is observed whenever the sublevels of the BE triplet are brought into coincidence by applying an external perturbation, e.g., a magnetic field, provided that there exist some static interactions coupling the close approaching sublevels, and that there exists some inequivalency between these levels due to the steady-state excitation mechanism (different generation rates and/or different recombination rates), which leads to a difference in their populations. In the vicinity of the avoided crossing point the approaching levels repel each other and strong mixing of their wave functions occurs, which is manifested by a resonantlike variation either in the total photoluminescence intensity, or more sensitively in the polarization of the emitted light (due to the BE recombination). It is illustrated that an unthermalized BE triplet exhibits stronger LAC effects, in comparison with a thermalized BE triplet. Characteristic fingerprints for these two types of BE triplets are shown to exist in the high magnetic field region, where the thermalized BE triplet displays stronger field-dependent features than the unthermalized BE triplet. The origins of the static interactions responsible for the LAC effects could be the Zeeman, fine-structure, and hyperfine interactions, but has been argued to be dominated by the hyperfine interactions, for the examples studied. Good agreement has been obtained between the present theoretical expectations and experimental observations for complex defects in GaP. It is shown that this simple steady-state LAC spectroscopy in complete absence of perturbing radiofrequency or microwave fields provides useful information of the BE states, including, e.g., the fine-structure and hyperfine-structure interactions, g factors, symmetry, mixing of the substates, as well as the thermal behavior of the BE and its associated defect.

ACKNOWLEDGMENTS

We acknowledge discussions with F. P. Wang.

*Permanent address: Institute of Physics, Polish Academy of Sciences, al. Lotnikow 32/46, PL-02-668 Warsaw, Poland.

[1]M. Goldman, *Spin Temperature and Nuclear Magnetic Resonance in Solids* (Oxford University, London, 1970).

[2]For a review, see, e.g., D. H. Levy, in *Advances in Magnetic Resonance,* edited by J. S. Waugh (Academic, New York, 1973), Vol. 6, p. 1.

[3]H. J. Beyer and H. Kleinpoppen, in *Progress in Atomic Spectroscopy,* edited by W. Hanle and H. Kleinpoppen (Plenum, New York, 1978), Part A, pp. 607–637.

[4]V. Macho, J. P. Colpa, and D. Stehlike, Chem. Phys. **44**, 113 (1979).

[5]L. Benthem, J. H. Lichtenbelt, and D. A. Wiersma, Chem. Phys. **29**, 367 (1978).

[6]J. A. Mucha and D. W. Pratt, J. Chem. Phys. **66**, 5356 (1977).

[7]D. H. Levy, J. Chem. Phys. **56**, 5493 (1972).

[8]T. A. Miller, J. Chem. Phys. **58**, 2358 (1973).

[9]L. T. Cheng and A. L. Kwiram, Chem. Phys. Lett. **4**, 457 (1969).

[10]H. Sixl and M. Schwoerer, Chem. Phys. Lett. **6**, 21 (1970).

[11]W. S. Veeman and J. H. van der Waals, Chem. Phys. Lett. **7**, 65 (1970).

[12]H. Veenvliet and D. A. Wiersma, J. Chem. Phys. **60**, 704 (1974).

[13]T. G. Eck, L. L. Foldy, and H. Wieder, Phys. Rev. Lett. **10**, 239 (1963).

[14]K. M. Lee, Le Si Dang, and G. D. Watkins, Solid State Commun. **37**, 551 (1981).

[15]H. P. Gislason, B. Monemar, P. J. Dean, D. C. Herbert, S. Depinna, B. C. Cavenett, and N. Killoran, Phys. Rev. B **26**, 827 (1982).

[16]A. Kana-ah, B. C. Cavenett, H. P. Gislason, B. Monemar, and M. E. Pistol, J. Phys. C **19**, 1239 (1986).

[17]W. M. Chen, B. Monemar, and M. Godlewski, Phys. Rev. B **37**, 2564 (1988).

[18]W. M. Chen and B. Monemar, Phys. Rev. B **38**, 12 660 (1988).

[19]In the present paper, we mean by the notation "neutral isoelectronic complex defects" such complex defects which have an electrically neutral ground state with no electronic particles bound.

[20]B. Monemar, U. Lindefelt, and M. E. Pistol, J. Lumin. **36**, 149 (1986).

[21]W. M. Chen, B. Monemar, and M. Godlewski, in *Defect and Diffusion Forum,* edited by H. J. von Bardeleben (Trans Tech, Aedermannsdorf, 1989), Vol. 62/63, p. 133.

[22]K. Morigake, Jpn. J. Appl. Phys. **22**, 375 (1983).

[23]M. Godlewski, W. M. Chen, and B. Monemar, Phys. Rev. B **37**, 8795 (1988).

[24]A. Abragam and B. Bleany, *Electron Paramagnetic Resonance of Transition Ions* (Clarendon, Oxford, 1970); B. Monemar, W. M. Chen, and M. Godlewski, Mater. Sci. Forum Vols. 38–41, 769 (1989).

[25]The basis wave functions $|S,M\rangle$ are directly related to the zero-(magnetic)-field eigenstates of the BE-triplet sublevels for a given defect. The sense of polarization for these sublevels is uniquely determined by the defect symmetry, however. The degree of the polarization, on the other hand, is governed by the coupling to their excited states, via various perturbations such as spin-orbit interaction and electron-nuclear coupling, since the electric-dipole transition between a pure spin triplet and its spin-singlet ground state is generally believed to be spin forbidden.

[26]In the numerical calculations and the discussions below, it is assumed that the polarizations of the triplet sublevels have a direct one-to-one correspondence to the basis spin states, i.e., $\sigma+$ for $|1,+1\rangle$, $\sigma-$ for $|1,-1\rangle$, and π for $|1,0\rangle$. This is done for the sake of simplicity, and is not necessarily true for every specific BE triplet. The sense of polarization in correlation with the spin state is in general very different from case to case, due to variations in the orbital part of the wave function and the mixing with excited states. Furthermore, the theoretical illustrations in this work are mainly focused on the LAC effect on the $L_{\sigma-}-L_{\sigma+}$ PL signal. It is quite straightforward, however, to extend these discussions to the LAC effect on the total PL intensity.

[27]B. Monemar, H. P. Gislason, P. J. Dean, and D. C. Herbert, Phys. Rev. B **25**, 7719 (1982).

[28]W. M. Chen, B. Monemar, and M. Godlewski, Phys. Rev. B **39**, 3153 (1989).

[29]W. M. Chen, H. P. Gislason, and B. Monemar, Phys. Rev. B **36**, 5058 (1987).

[30]P. J. Dean, Solid State Commun. **9**, 2211 (1971).